AtALMT9 is a malate-activated vacuolar chloride channel required for stomatal opening in Arabidopsis

Alexis De Angeli, Jingbo Zhang, Stefan Meyer and Enrico Martinoia

Supplementary Figures

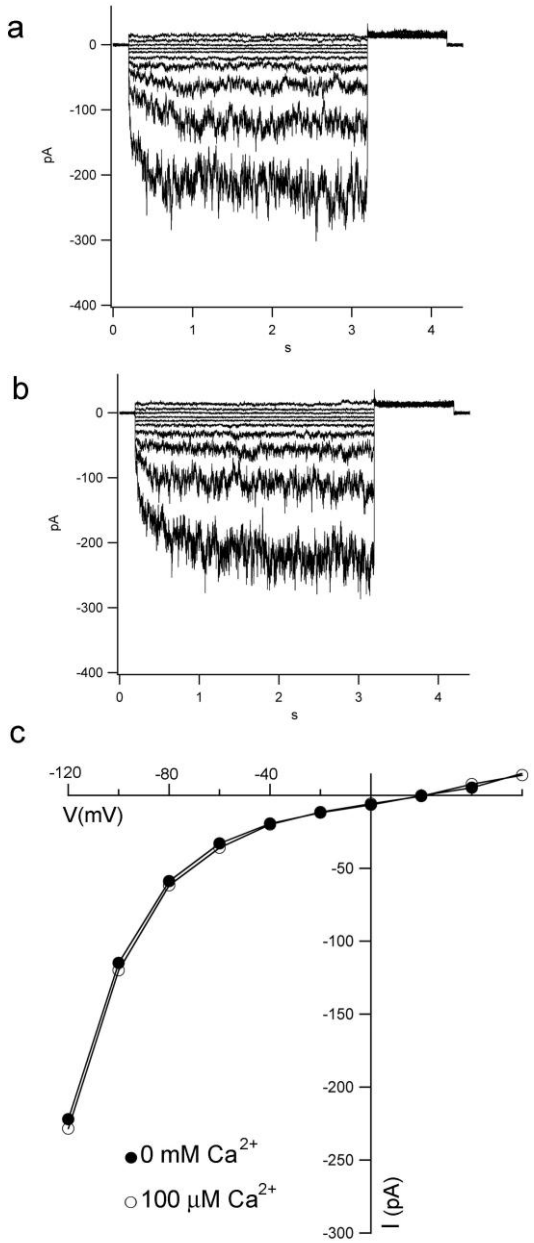

Supplementary Figure S1. Cytosolic Ca^{2+} does not activate AtALMT9 mediated chloride currents. (**a**,**b**) Typical excised cytosolic-side-out patch current form *N. benthamiana* AtALMT9 overexpressing vacuoles in nominal absence of cytosolic calcium (0 mM Ca^{2+}; **a**) and after perfusion with 100 µM cytosolic Ca^{2+} (**b**). (**c**), I/V curves of the total currents from (**a)** and (**b**). The mean ratio is $I_{Ca}/I_{0.1mM\ Ca}$= 1.1 ± 0.1 at -120 mV (n=3). The 0 mM Ca^{2+} *cytosolic solution* contains: 100 mM HCl, 3 mM $MgCl_2$, 5mM EGTA, adjusted to pH 7.5 with BisTrisPropane. The 100 µM Ca^{2+} *cytosolic solution* contains: 100 mM HCl, 3 mM $MgCl_2$, 0.1 mM $CaCl_2$, adjusted to pH 7.5 with BisTrisPropane. *Vacuolar side solution*: 100 mM HCl, adjusted to pH 6 with BisTrisPropane. (**a**,**b**), from a holding potential of 0 mV a series of test voltages from +60 to -120 mV in steps of -20 mV was applied; tail potential -60 mV. Error bars are s.e.m. (**a**, **b**) Currents evoked in response 3s pulse from +60 mV to -120 mV in -20 mV steps, followed by a tail pulse at -60 mV, holding potential +60 mV.

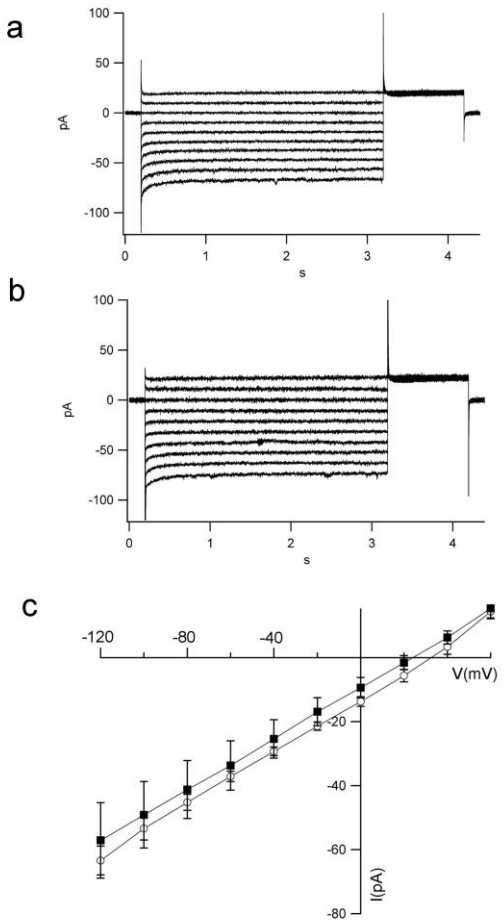

Supplementary Figure S2. Cytosolic malate does not activate chloride currents in excised cytosolic-side-out in patches from empty vector transformed vacuoles. (**a**,**b**) Typical excised cytosolic-side-out patch currents form *N. benthamiana* vacuoles obtained from empty-vector (pART27) transformed protoplasts. (**a**), currents recorded with a 100 mM Cl^-_{cyt} buffer and (**b**) after perfusion with 100 mM Cl^-_{cyt} + 1 mM $malate_{cyt}$ buffer. (**c**), mean I-V curves from currents recorded with a 100 mM Cl^-_{cyt} buffer and after perfusion with 100 mM Cl^-_{cyt} + 1 mM $malate_{cyt}$ buffer (n=6). *Vacuolar side solution*: 100 mM HCl, adjusted to pH 6 with BisTrisPropane. *Cytosolic side buffers*: 100 mM HCl, 3 mM $MgCl_2$, 0.1 mM $CaCl_2$, adjusted to pH 7.5 with BisTrisPropane; 100 mM HCl, 1 mM malic acid, 3 mM $MgCl_2$, 0.1 mM $CaCl_2$, adjusted to pH 7.5 with BisTrisPropane. Error bars are s.e.m. (**a**, **b**)Currents evoked in response 3s pulse from +60 mV to -120 mV in -20 mV steps, followed by a tail pulse at -60 mV, holding potential +60 mV.

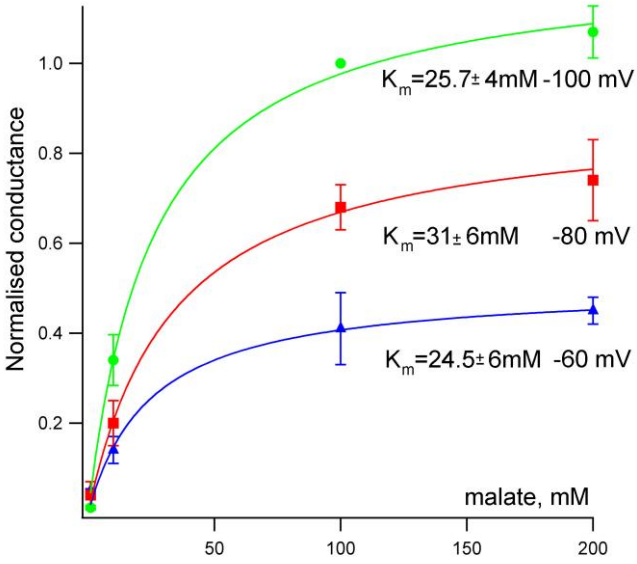

Supplementary Figure S3. Conductance of *At*ALMT9 currents as a function of cytosolic malate concentration measured at different membrane potentials as indicated. The data were normalised to the conductance in 100 mM malate$_{cyt}$ at -100 mV and fitted with a Michaelis-Menten function. The results indicate that the K_m is voltage independent and exhibits a mean value of 27 mM malate.

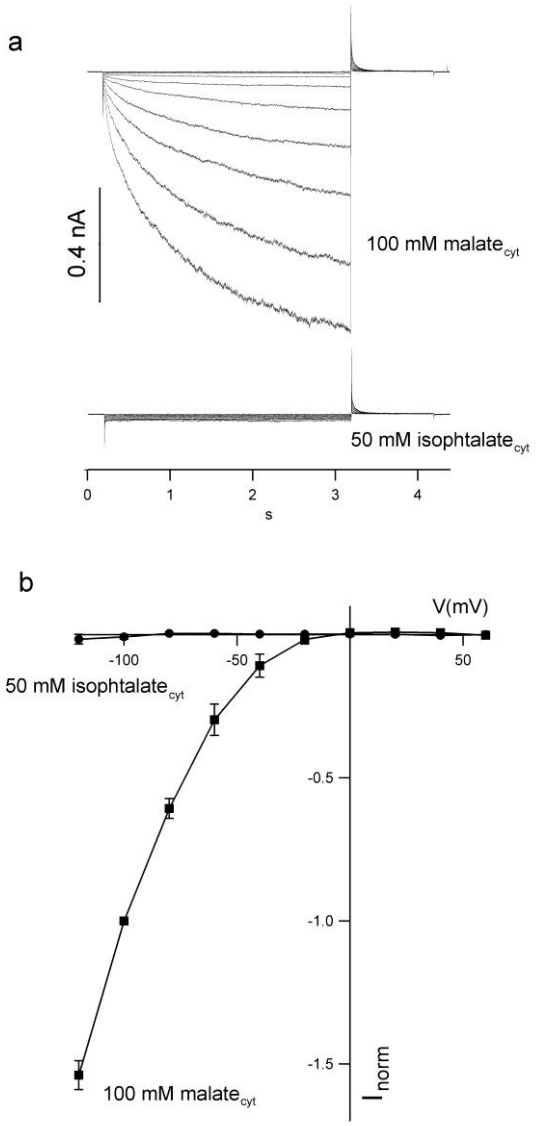

Supplementary Figure S4. Isophtalic acid is not permeable through *At*ALMT9. (a) Representative *At*ALMT9 currents recorded with voltage pulses form 40 to -120 mV in presence of 100 mM malate$_{cyt}$ and 50 mM isophtalate$_{cyt}$. **(b)** Normalised mean IV curves in presence of 100 mM malate$_{cyt}$ and 50 mM isophtalate$_{cyt}$. The currents detected in the presence of isophtalate$_{cyt}$ correspond to 1% at -120 mV of the currents measured in presence of malate. The pipette solutions was: 112 mM malic acid, 5 mM HCl, adjusted with BisTrisPropane to pH 6; the cytosolic solution were: i) 100 mM malic acid, 3 mM $MgCl_2$, 0.1 mM $CaCl_2$, adjusted to pH 7.5 with BisTrisPropane; ii) 50 mM isophtalic acid, 3 mM $MgCl_2$, 0.1 mM $CaCl_2$, adjusted to pH 7.5 with BisTrisPropane. (**a**, **b**) Currents evoked in response 3s pulse from +60 mV to -120 mV in -20 mV steps, followed by a tail pulse at -60 mV, holding potential +60 mV.

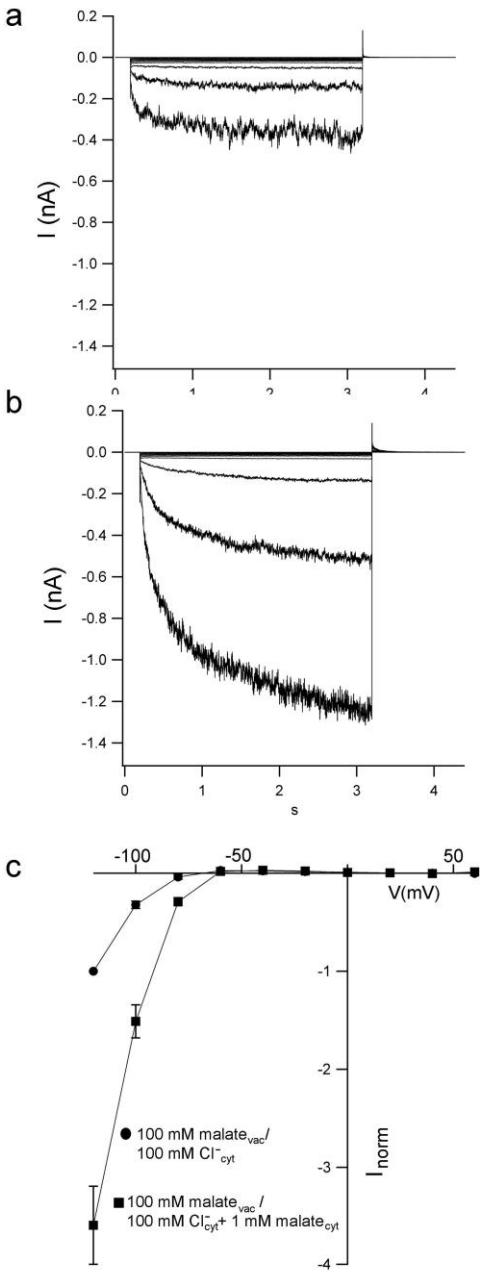

Supplementary Figure S5. Cytosolic malate activates AtALMT9 chloride currents even in presence of 100 mM malate in the vacuolar buffer. (**a**,**b**), Typical excised cytosolic-side-out patch current form *N. benthamiana* AtALMT9 overexpressing vacuoles with 100 mM malate in the vacuolar buffer and 100 mM Cl^-_{cyt} (**a**) and after perfusion with 100 mM Cl^-_{cyt} + 1 mM $malate_{cyt}$ (**b**). (**c**), mean normalised I/V curves of the time dependent currents from (**a)** and (**b**). In presence of 100 mM $malate_{vac}$ the mean ratio $I^{1mal,\ 100\ Cl-}_{cyt}/I^{100\ Cl-}_{cyt}$= 3.6 ± 0.4 at -120 mV. *Cytosolic side buffers*: 100 mM HCl, 3 mM $MgCl_2$, 0.1 mM $CaCl_2$, adjusted to pH 7.5 with BisTrisPropane; 100 mM HCl, 1 mM malic acid, 3 mM $MgCl_2$, 0.1 mM $CaCl_2$, adjusted to pH 7.5 with BisTrisPropane. *Vacuolar side buffer*: 112 mM malic acid, 5 mM HCl, adjuste with BisTrisPropane, pH 6. (**a**,**b, c**), from a holding potential of -60 mV a series of test voltages from +60 to -120 mV in steps of -20 mV was applied; tail potential -60 mV. Error bars are s.e.m. (**a**, **b**) Currents evoked in response 3s pulse from +60 mV to -120 mV in -20 mV steps, followed by a tail pulse at -60 mV, holding potential +60 mV.

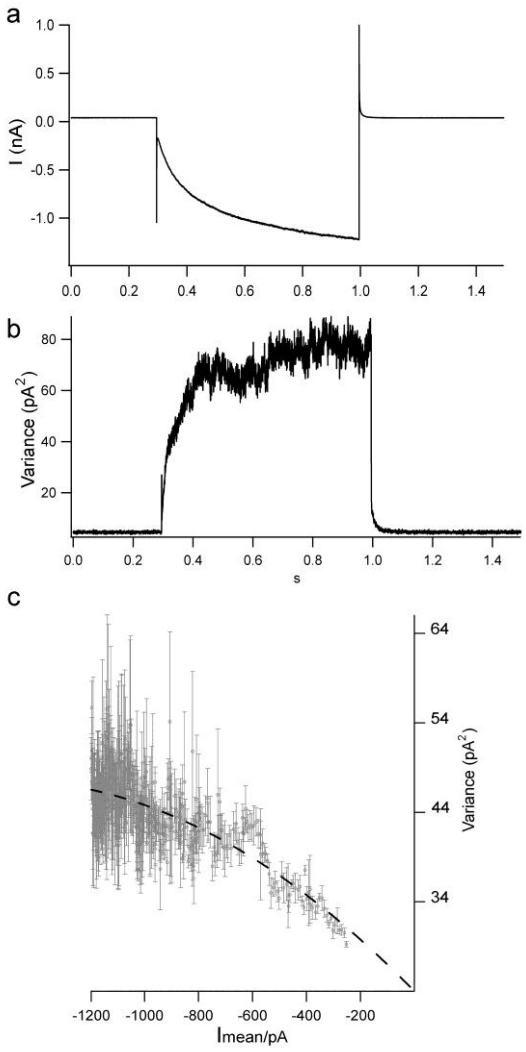

Supplementary Figure S6. Non stationary noise analysis of *At*ALMT9 in excised cytosolic side-out patches. (**a**) Average of 100 macroscopic current recordings and (**b**) corresponding variance from a representative patch recorded at -120 mV. (**c**) Plot of the variance against the corresponding mean current from the same patch as in (**a)**. To estimate the unitary channel current amplitude the variance mean relationship was fitted with the following equation:

$$\sigma^2 = i < I > - \frac{< I >^2}{N}$$

where σ^2 is the variance, i the unitary channel current, <I> is the mean current and N the number of channels in the patch. The mean unitary current amplitude was estimated to be -3.4±0.8 pA at -120 mV (n=3). Data were filtered at 10 kHz and sampled at 5 kHz.

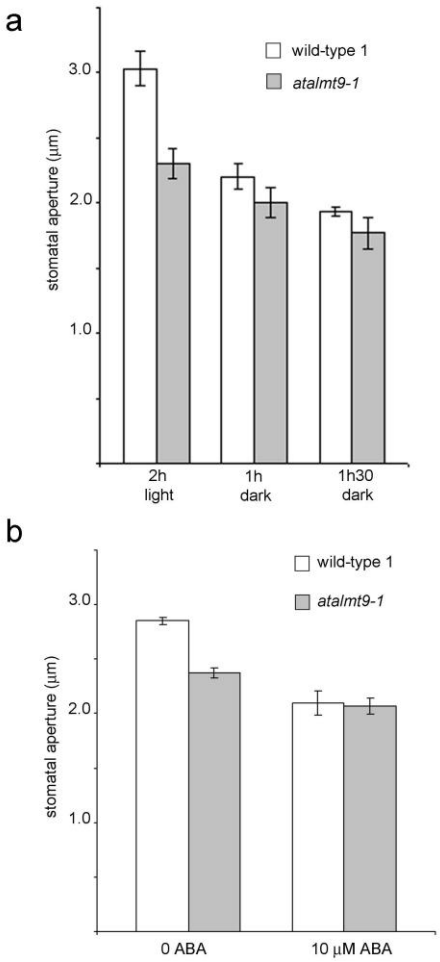

Supplementary Figure S7. AtALMT9 is not involved in triggering stomata closure in response to dark and ABA. (**a**), stomatal aperture were measured after 2h light in 30 mM KCl, after epidermal strips were transferred in the dark and stomatal aperture was measured after 1h and 1h30. In both wild-type (n=4) and *atalmt9-1* knock-out (n=4) the closure was statistically significant (wild-type 1 P=0.03; *atalmt9-1* P=0.01) and close to the same extent. (**b**), stomatal aperture were measured after 2h light in 30 mM KCl, subsequently 10 µM ABA was added and stomata aperture measured after 2h incubation in the light. In both wild-type (n=4) and *atalmt9-1* knock-out (n=4) the closure was statistically significant (wild-type 1 P=0.003; *atalmt9-1* P=0.009) and close to the same extent. In (**a**) and (**b**) the opening buffer was 30 mM KCl, 5 mM MES, 0.1 mM $CaCl_2$, pH 5.7. Error bars are s.e.m.

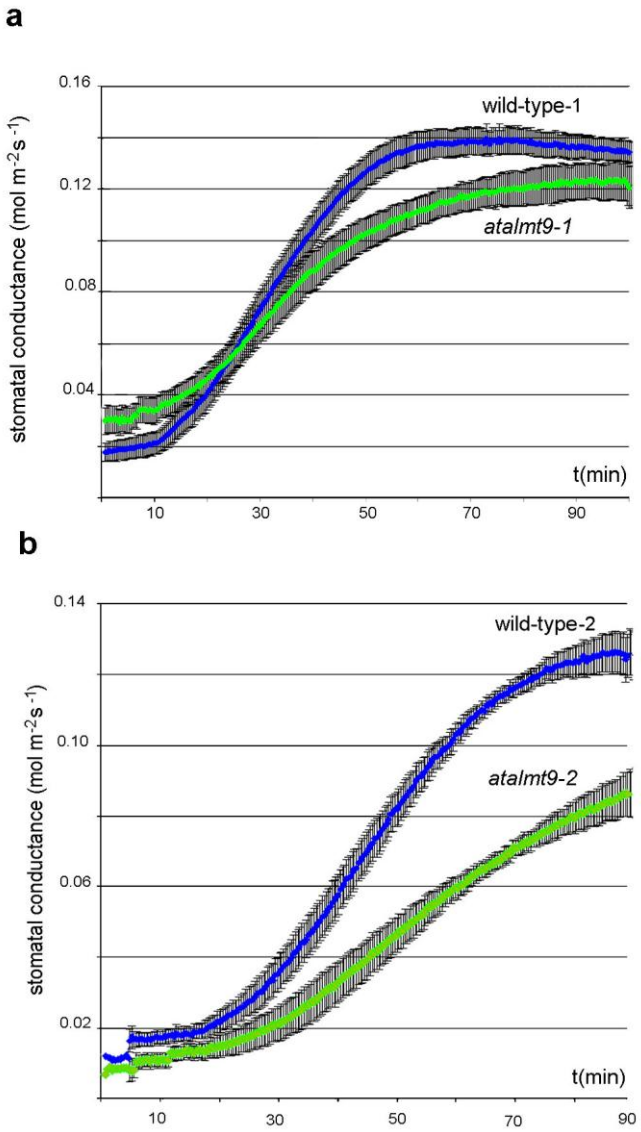

Supplementary Figure S8. Time course of the mean stomata conductance during light-induced opening in a second independent batch of plant. Measurements were performed using a LI-6400; LI-COR gas exchange chamber as in Figure 4d. **(a)** wild-type1 n=9 plants, *atalmt9-1* n=8. **(b)** wild-type n=6, *atalmt9-2* n=8 plants. Error bars represent s.e.m.

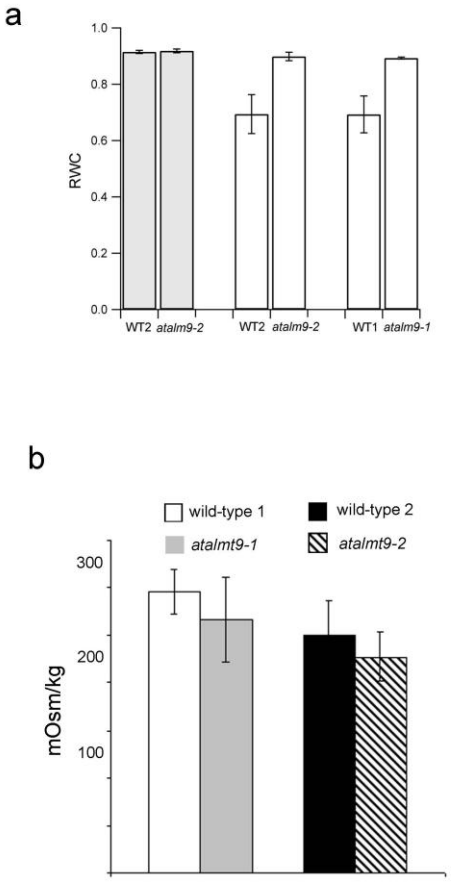

Supplementary Figure S9. (**a**), **Relative water content and osmolarity in wild-type and atalmt9 mutant plants**. Histograms showing the relative water content (RWC) of *atalmt9-1*, *atalmt9-2* and the corresponding wild-type plants before (*atalmt9-2* and corresponding wild-type, grey bars) and 8 days after stopping watering (empty bars). Wild-type plants exhibited a 23% larger water loss compared to the corresponding knockout lines. For each genotype at least 10 different rosettes were used to determine the relative water content. The RWC was calculated with the following equation: RWC=(FW-DW)/FW, FW is fresh weight and DW is dry weight. (**b**), Osmolarity of the leaf sap extracted from *A. thaliana* rosette leaves. Leaves undergo a cycle of freezing/thawing and subsequently were mechanically grinded. After centrifugation the supernatant was collected and used for osmolarity measurements with a micro-osmometer. For each genotype 8 plants were used. No significant difference was observed between wild-types and mutants. Error bars represent s.e.m.

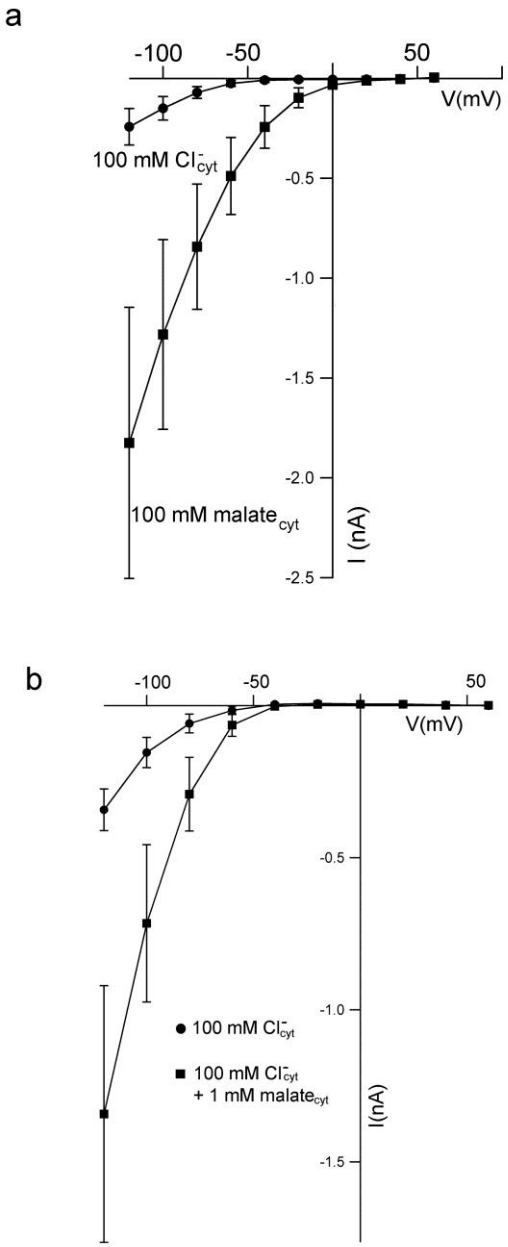

Supplementary Figure S10. (**a**), **Non-normalised I-V curves from Fig 1 b**. *Vacuolar side buffer*: 112 mM malic acid, 5 mM HCl, adjuste with BisTrisPropane, pH 6. *Cytosolic side buffers*: 100 mM HCl, 3 mM $MgCl_2$, 0.1 mM $CaCl_2$, adjusted to pH 7.5 with BisTrisPropane; 100 mM malic acid, 3 mM $MgCl_2$, 0.1 mM $CaCl_2$, adjusted to pH 7.5 with BisTrisPropane. (**b**), **non normalised I-V curves from Fig 1 b**. *Cytosolic side buffers*: 100 mM HCl, 3 mM $MgCl_2$, 0.1 mM $CaCl_2$, adjusted to pH 7.5 with BisTrisPropane; 100 mM HCl, 1 mM malic acid, 3 mM $MgCl_2$, 0.1 mM $CaCl_2$, adjusted to pH 7.5 with BisTrisPropane. *Vacuolar side buffer*: 100 mM HCl, adjusted to pH 6 with BisTrisPropane. Error bars are s.e.m.